
The Antarctic Atmosphere as Seen by Satellites

J. J. Barnett

Phil. Trans. R. Soc. Lond. B 1977 **279**, 247-259

doi: 10.1098/rstb.1977.0087

Email alerting service

Receive free email alerts when new articles cite this article - sign up in the box at the top right-hand corner of the article or click [here](#)

The Antarctic atmosphere as seen by satellites

BY J. J. BARNETT

Department of Atmospheric Physics, Clarendon Laboratory, University of Oxford

A brief review is given of satellite observations of the atmosphere which are relevant to Antarctic studies. Aspects of the behaviour of the Southern Hemisphere during winter are described using Nimbus selective chopper radiometer and pressure modulator radiometer temperature sounding data which extend to mesopause levels. Emphasis is placed upon the new measurements of the mesosphere, and monthly mean Southern Hemisphere maps are given for various heights in the mesosphere during August 1975 and for the months July–September 1975 for the top level near the mesopause. Planetary waves in the Southern Hemisphere are found to propagate to the mesopause with diminution of the temperature amplitude above about the stratopause, and tilt westward with increasing height and decreasing latitude.

INTRODUCTION

Satellite observations have advanced substantially since Tiros 1 took the first television pictures of the atmosphere in 1960. These advances have been especially valuable in the Southern Hemisphere where conventional ground-based observations are sparse. In contrast one of the problems with satellite data is their abundance and using them is difficult unless they have been suitably condensed – often not the case with experimental instruments. The first part of this paper describes some of the types of data available from satellites and relevant to the study of the antarctic atmosphere, while the second part gives a more detailed account of the behaviour of the Southern Hemisphere stratosphere and mesosphere as observed by the selective chopper radiometer (s.c.r.) and pressure modulator radiometer (p.m.r.) temperature sounding instruments.

1.1 *Imaging devices*

Visible and infrared imaging from satellites are both relatively advanced. Visible pictures are only useful when taken in daylight, which excludes observation during polar night. A further problem is that snow, ice and cloud appear similar, making interpretation difficult near the poles. Infrared imaging devices normally measure thermal emission in the 3.5–4.1 or 10.5–12.5 μm window regions where the atmosphere is nearly transparent, and therefore receive radiation from either the surface, or the cloud top where clouds are present. The measured radiation I is given by

$$I = \epsilon B(T), \quad (1)$$

where ϵ is emissivity (normally taken as 1) and $B(T)$ is the Planck function at temperature T . Detail is seen only by virtue of temperature contrasts; cloud tops are normally colder than the surface, but isothermal profiles can occur over the polar caps and cause difficulty in distinguishing cloud from surface. The height of the cloud top can be deduced from the observed temperature when the temperature profile is known and varies sufficiently rapidly with height.

Polar imaging is normally done from high inclination orbits since geostationary (equatorial orbit) satellites give little information poleward of 60° latitude. The NOAA-3 and NOAA-4

satellites show the current state-of-art of operational satellites (Krishna Rao & McClain 1974). Each carries a scanning radiometer which measures at 0.55–0.75 μm (visible) and 10.5–12.5 μm (infrared) with an 8 km resolution scanning pattern, and a very high resolution radiometer measuring in similar spectral regions with 1 km resolution. The latter data are transmitted in real-time for reception by ground stations within line-of-sight, the data rate being so high that only a few minutes per orbit can be stored onboard.

1.2 *Observations of the surface*

The surface has a very strong influence on the behaviour of the atmosphere. Over most of the globe the land and sea have fixed areas, but near the poles the formation of ice, which is under the control of the atmosphere, causes those areas to vary. Over the oceans ice cover provides an insulating blanket, preventing upward heat flux and allowing the atmosphere to cool to very low temperatures in winter. Snow and ice have a very high albedo, so little solar radiation is absorbed at the surface, reducing the heating of the low atmosphere and the melting of the ice. Both the maximum area of pack-ice cover and its seasonal variation are very much larger in the Southern Hemisphere than in the Northern Hemisphere, the ranges being approximately 2.6–18.8 and 9.5–12.5 $\times 10^6$ km² respectively (Fletcher 1975), showing the importance of ice cover studies near Antarctica.

Television pictures show the surface where not obscured by cloud, and sequences of pictures over the same location can be processed by computer to retain just those features which recur at the same location, usually surface features.

Infrared window observations of the surface are used to map sea surface temperature, recognized by the high and repeatable temperatures then observed, most areas being clear of cloud at some time during a collection period of several days. Accuracy is limited to 1–2 °C by atmospheric water vapour absorption.

The Nimbus 5 and Nimbus 6 satellites carried the electrical scanning microwave radiometers which measure thermal emission at wavelengths near 1.55 and 0.81 cm respectively. Both the atmosphere and clouds are transparent at these wavelengths, so emission is from the surface. Equation (1) applies but the measurements are primarily of varying emissivity, which is typically 0.4 for open sea, 0.95 for new ice and 0.8 for old ice (Gloersen *et al.* 1974). These are much larger than the variations of the Planck function, which is proportional to temperature (approx. 200–290 K) at these wavelengths. These observations are excellent for ice mapping, with a very high ice-sea contrast, the sea having an apparent temperature of about 110 K.

The Landsat satellites (previously called ERTS) take very high resolution images (0.1 km) in various spectral regions, but passes over the same area are at intervals of 18 days which is too infrequent for most meteorological applications.

1.3 *Observations of the troposphere*

Cloud pictures give a detailed view of tropospheric disturbances and are valuable for short-term forecasting and for general scientific studies (figure 1).

Measurements of radiation emerging vertically from the atmosphere at wavelengths in the vicinity of spectral lines of a uniformly mixed gas yield information about the temperature structure of the atmosphere. Radiation at each wavelength originates as thermal emission in a layer 10–20 km thick, at a height dependent on the wavelength, and gives a measure of the temperature of that layer (Houghton & Smith 1970). Sophisticated techniques allow measurements

from layers centred from near the surface to 85 km altitude. The Nimbus 6 satellite has approximately 19 such channels measuring emission in the $4.3 \mu\text{m}$ and $15 \mu\text{m}$ bands of carbon dioxide, in the 5 mm microwave band of oxygen and in various spectral windows. Microwave channels have the advantage of seeing through cloud (although not heavy rain, which they can be used to map), but there are problems because of varying surface emissivity when they

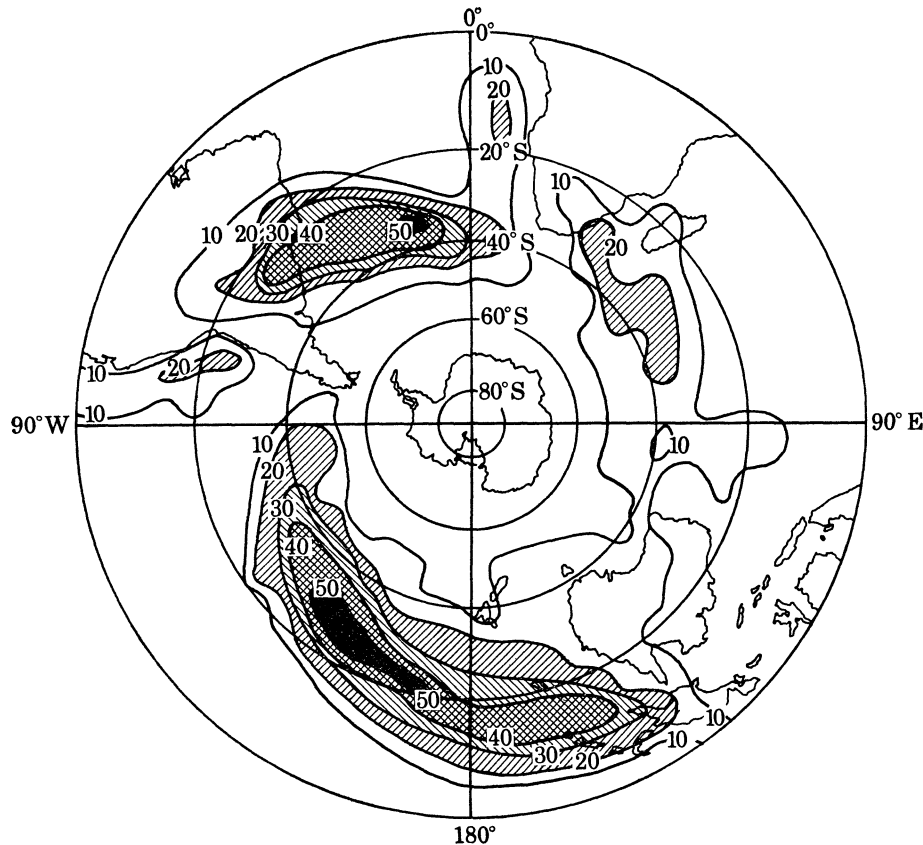


FIGURE 1. Average cloudiness shown by satellite. Percentage frequency of 5-day-averaged cloud mosaics having axes of major cloud bands within a 5° latitude by 10° longitude square for the whole period November 1968 to October 1971 (Streten 1973).

observe a layer extending down to near the surface. The tropospheric channels scan either side of the track with a 25 km diameter field of view. Derivation of temperatures ('retrieval') in the presence of cloud is a major problem, but joint use of scanning, of several different wavelengths in the infrared where the Planck function has different temperature variation and use of microwave channels promise to give good retrievals down to the surface except under continuous cloud cover. Other scanning infrared and microwave channels measure water vapour emission, allowing humidity to be mapped. Similar instruments will be carried by Tiros N operational satellites from 1978. Current operational sounders carry scanning (75 km resolution) infrared temperature sounders. Observations are routinely transmitted over the international meteorological communication circuits.

Wind at cloud heights can be deduced by observing cloud motions from a geostationary satellite, although this method is limited to tropical and mid latitudes. Another method involves tracking by satellite of balloons which float at a constant density level (normally about

200 mbar (20 kPa)) carrying radio transponders. In the Eole experiment (Morel & Bandeen 1973) balloons were released from Argentina and tracked with 1–2 km accuracy. Up to 280 balloons were operating at any one time, spread over most of the Southern Hemisphere. Although balloons made several circuits of the globe before failing (the average lifetime was 103 days), the running costs of such a system are high. However the Eole data have received extensive scientific analysis, the wind fields being used, *inter alia*, to calculate energy and momentum fluxes.

1.4 The net radiation budget

Various components of the Earth radiation budget have been monitored since 1959, but with increasingly sophisticated instruments. The most advanced measurements are being made by the Nimbus 6 Earth radiation budget experiment which measures outgoing radiation as functions of zenith angle and wavelength. Figure 2 shows the long-term means of absorbed and emitted radiation and albedo derived from measurements by Tiros, Essa and Nimbus spacecraft. The highest albedos and lowest outgoing fluxes are seen to occur over Antarctica.

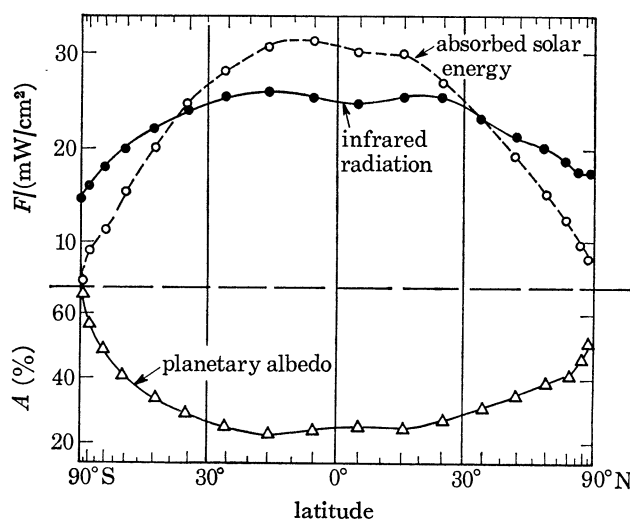


FIGURE 2. Components of the Earth's radiation budget over the period 1962–6. The abscissa is scaled by cosine of latitude so that the area of different parts of the curve is proportional to the total radiation in that latitude band (Vonder Haar & Suomi 1971).

1.5 Observations above the troposphere

Ozone mixing ratio above about 30 km and total ozone have been measured continuously since 1970 by the backscatter ultraviolet spectrometer carried by Nimbus 4 (Krueger, Heath & Mateer 1973). The instrument measures the intensity of solar ultraviolet emerging from the atmosphere, this radiation having been Rayleigh scattered by atmospheric gases at various levels and partially attenuated by ozone along the path. Measurements at several wavelengths enable a mixing ratio profile to be deduced with a vertical resolution of about 10 km. Moonlit observations are possible, but most of the results emerging are during sunlight, so excluding the polar night which is of great interest. Measurements in the 9.6 μm band of ozone by the Nimbus 3 and 4 infrared interferometer spectrometers have been used to map total ozone, although the method requires assumptions of the temperature or height of the ozone layer, and is very insensitive in the near isothermal conditions which may occur over Antarctica. The Nimbus 6

limb radiance inversion radiometer departed from previous practice by measuring emission from the limb, using cryogen cooled detectors (with an 8-month life) and a fast vertical scan to minimize attitude stability problems. $9.6 \mu\text{m}$ ozone, $15 \mu\text{m}$ carbon dioxide and $23\text{--}27 \mu\text{m}$ water vapour emission were measured to sound ozone mixing ratio, temperature and humidity with a vertical resolution of 3 km over a 15–65 km height range. Coverage was limited to 64°S – 83°N . Results appear good although data reduction is still at a preliminary stage.

Conventional nadir viewing spectrometers and filter radiometers enable temperature to be deduced (sounded) at heights up to about 30 km (10 mbar), although with rather poor vertical resolution above the tropopause. A wide variety of research has used these data; e.g. Adler (1975) derived a heat budget and the mean meridional circulation for both hemispheres during winter up to 10 mbar; Fritz & Soules (1972) studied sudden warmings and planetary waves in both hemispheres, Labitzke & Van Loon (1972) gave an extensive account of the behaviour of the Southern Hemisphere and used many satellite data.

2.1 *Temperature sounding of the stratosphere and mesosphere*

It is possible to sound temperature to high levels with a nadir sounding instrument by using carbon dioxide as a filter to give high spectral resolution. The selective chopper radiometers

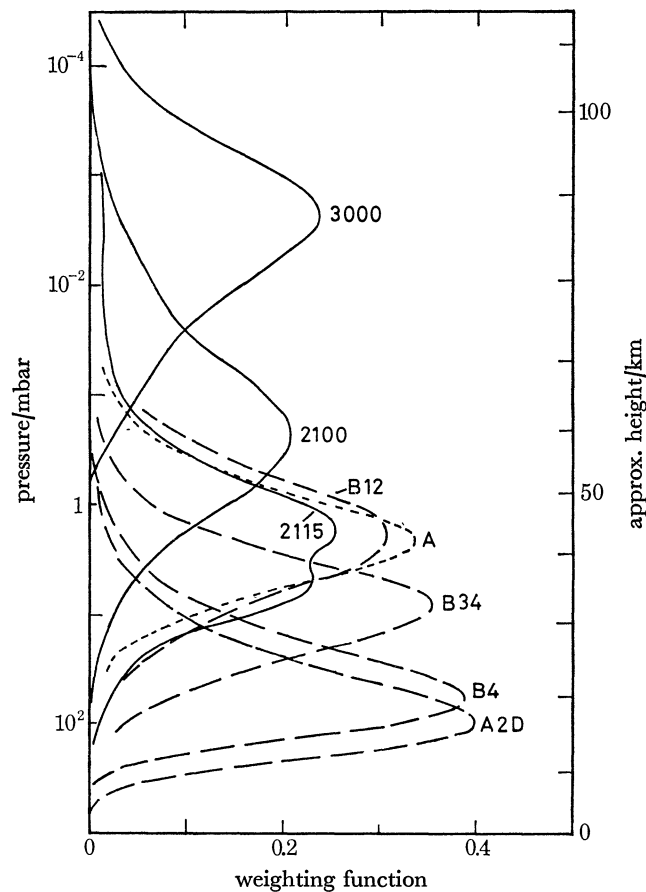


FIGURE 3. The weighting functions of channels of the s.c.r.s and p.m.r. referred to in the text. ---, Nimbus 4 s.c.r.; —, Nimbus 5 s.c.r.; —, Nimbus 6 p.m.r. The weighting function of Nimbus 5 channel B23 is intermediate between those of B12 and B34.

(s.c.r.) carried by Nimbus 4 and 5 (launched in 1970 and 1972) use single cells of carbon dioxide permanently in the beam to filter out the radiation in line centres and improve vertical resolution in the lower stratosphere. To measure at higher levels they passed radiation alternately through two cells containing CO₂ at different pressures, the difference signal being a measure of radiation at line centres, which originates in 15–20 km thick layers in the mid and

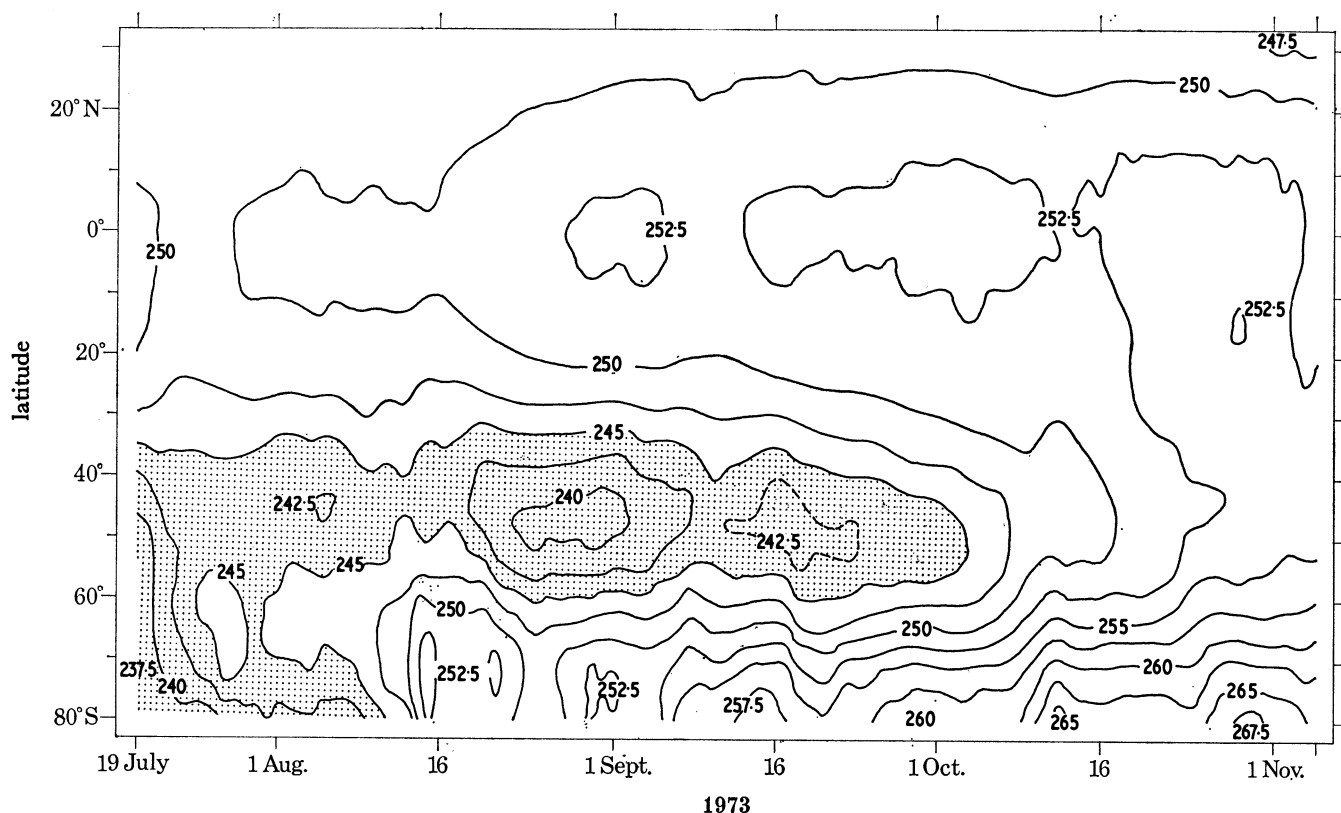


FIGURE 4. Temperature (K) equivalent to the zonal mean radiance measured by Nimbus 5 s.c.r. channel B12. The region colder than 245 K is dotted.

upper stratosphere. The Nimbus 6 pressure modulator radiometer (p.m.r.) employs two single CO₂ cells, each with a piston to modulate the pressure at about 15 Hz, to measure emission from layers in the upper stratosphere and mesosphere. Taking differences between the channels gives the radiation from a 20 km thick layer centred at about 85 km altitude. The p.m.r. channels scan along the direction of spacecraft travel, introducing a Doppler shift of up to several times the spectral resolution, and causing the layer from which radiation is selected to move down to about 45 km at the end of the scan. The weighting functions for these channels, giving the relative response to emission from each level, are given in figure 3. Curtis, Houghton, Peskett & Rodgers (1974) gave a description of the instrument.

Together these instruments have provided continuous data for the stratosphere since 1970. The Southern Hemisphere is very inactive during summer at these levels, and most interpretation has centred about planetary wave and associated sudden warming activity during autumn, winter and spring.

2.2 *The hot winter pole*

Barnett (1974) used Nimbus 4 s.c.r. data to show the behaviour of the zonal mean over a period of one year (1970–1) at levels throughout the stratosphere. Probably the most interesting result which emerged for the Southern Hemisphere was the occurrence of a relatively hot south polar region with cold mid-latitudes at the highest level (about 2 mbar, 43 km) during late winter and spring. This behaviour has been confirmed during every Southern Hemisphere winter observed by the s.c.r.s and p.m.r. Figure 4 gives corresponding measurements during 1973. Behaviour is quite different in the Northern Hemisphere: variations are much bigger (more intense sudden warmings) and mask any tendency for a mid-latitude cold region to be present, although one sometimes emerges if zonal mean temperatures are averaged over a long period. Figure 5 shows the same effects at various levels during July and September. The winter pole is hot near the mesopause, as has long been known, but there is a slight minimum at about 20° S. The South Pole is very cold in the lower stratosphere, while at intermediate heights in

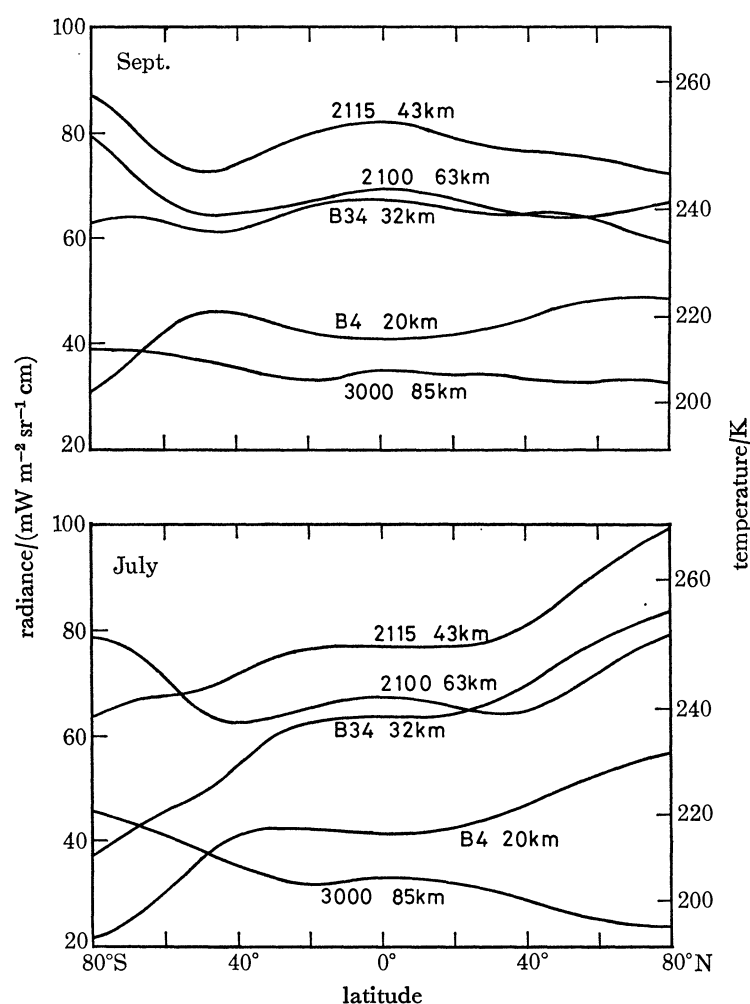


FIGURE 5. Variation of temperature with latitude and height: zonal mean radiance and equivalent temperature for various channels during July and September. 1974 data are used for channels B4 and B34; 1975 data are used for channels 2115, 2100 and 3000.

September and just in the mid-mesosphere (63 km) during July, the pole seems to follow the behaviour of the mesopause, being relatively hot (hotter than any other latitude at 43 km in September) while mid-latitudes show a pronounced minimum, in contrast to the maximum in both months at 20 km.

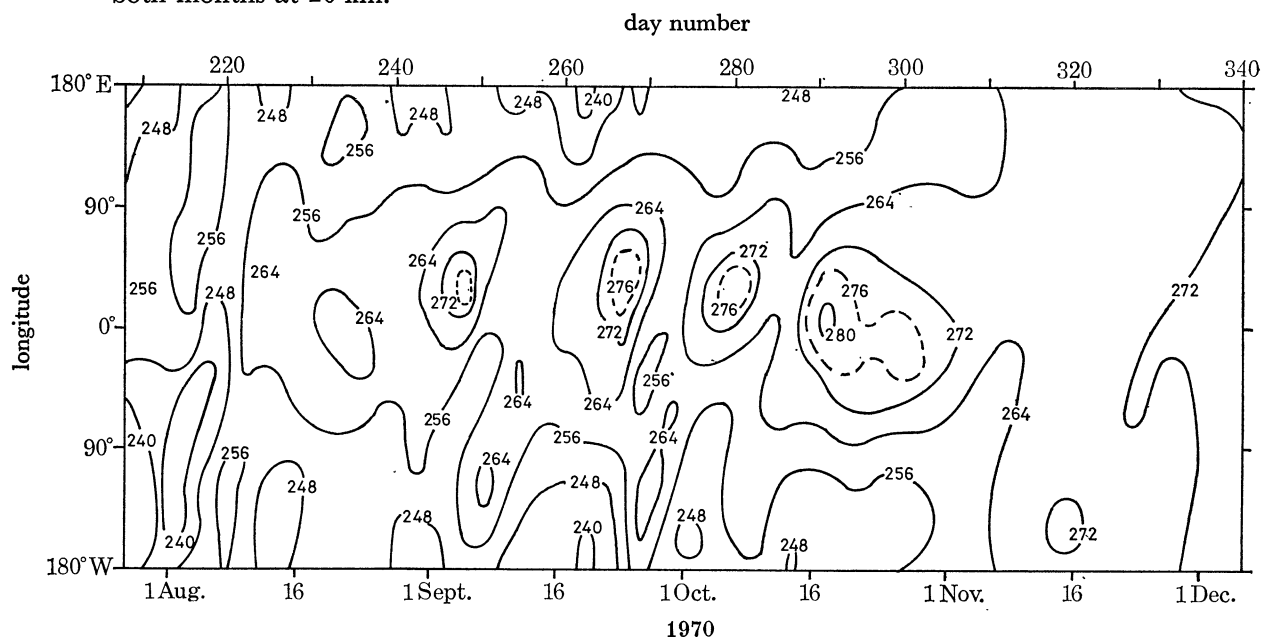


FIGURE 6. Wave pattern changes with time near 43 km given by time-longitude section around 64° S of the Nimbus 4 channel A radiance-equivalent temperature (K).

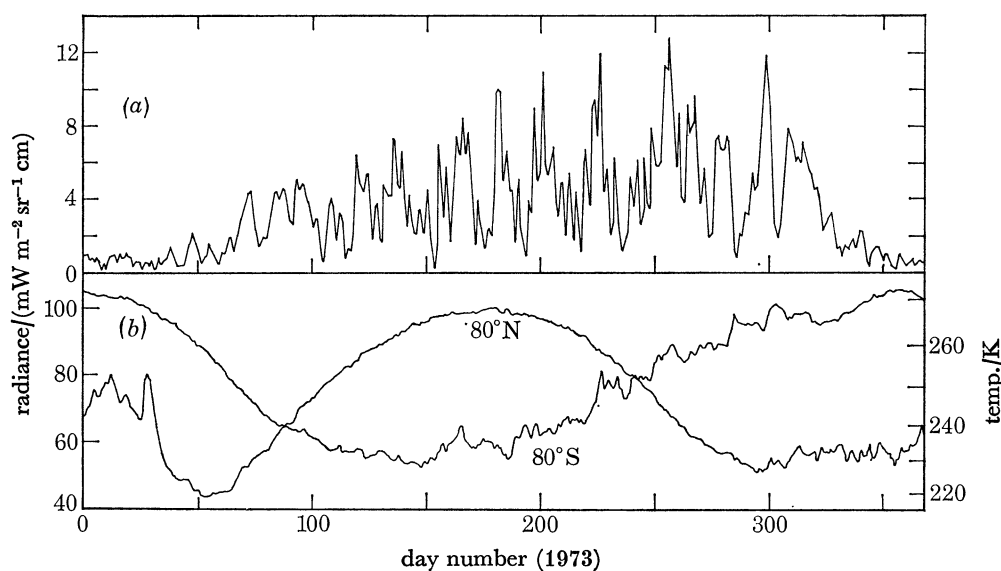


FIGURE 7. Nimbus 5 channel B12 (a) wavenumber one amplitude at 64° S; an interval of one radiance unit corresponds to about 0.8 K in this case; (b) zonal mean radiance at 80° N and 80° S.

2.3 Eddies during winter

Although rather less active in winter than the Northern Hemisphere, the Southern Hemisphere is no more predictable. Harwood (1975) showed how the wave pattern during the 1971

winter rotated about the South Pole three times between July and October. The pattern was primarily of wavenumber two and travelled eastwards at 15° longitude per day. This happened at all levels, but was most pronounced in the lower stratosphere. During 1970 however the pattern was stationary, of wavenumber one (offset vortex) and varying amplitude (figure 6). A series of warmings occurred at about 2-week intervals south of Africa with corresponding coolings over the Pacific, but with some evidence of superimposed waves travelling eastward. Chapman *et al.* (1974) used spectral analysis techniques to isolate individual stationary and travelling waves, and found that the wavenumber two component of the s.c.r. radiance field at 60° S during September and October 1970 progressed eastward at 14° longitude per day, in good agreement with the value given by Harwood. Figure 7*a* shows another series of eddy maxima during 1973, with peaks at 2–3 week intervals throughout the winter. Most of these

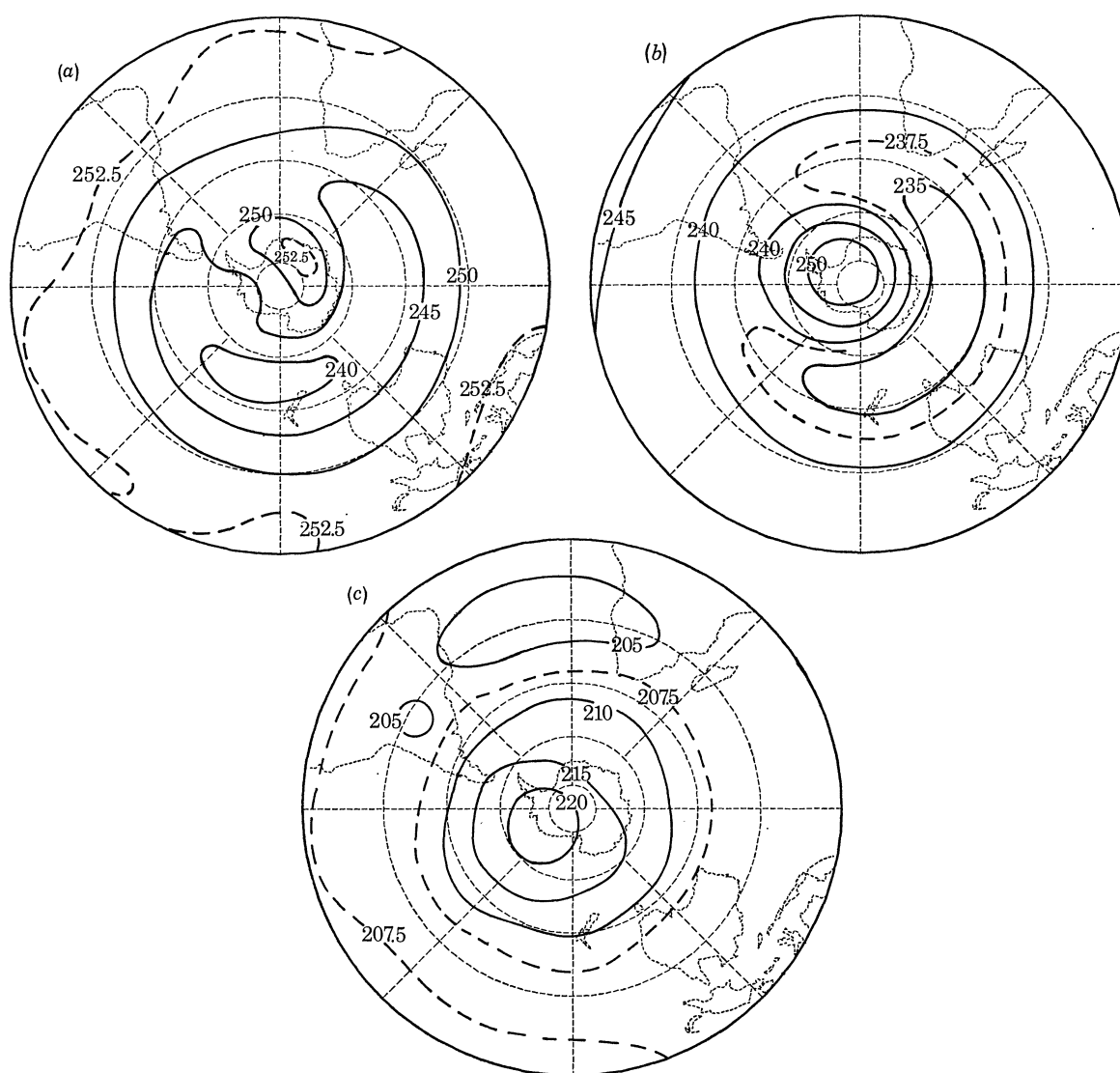


FIGURE 8. Three-dimensional structure of temperature field as shown by Southern Hemisphere polar stereographic maps of the temperature (K) equivalent to the August 1975 mean radiance measured by channels (a) 2115 (~ 43 km), (b) 2100 (~ 63 km) and (c) 3000 (~ 87 km).

peaks would be classified as minor warmings and several coincided with peaks of temperature near the South Pole, as shown in figure 7*b*. This behaviour is consistent with theory and calculation since winter planetary waves are known to transport heat polewards, and with observations by Harwood (1975) and Barnett (1975*b*). The latter paper described what is still the largest Southern Hemisphere warming observed from the s.c.r.s or p.m.r. Eddy amplitude had a maximum on 26 July 1974 when the peak-to-peak channel B23 brightness temperature variation around the 60° S latitude circle was over 40 K; (this variation was still less than two-thirds of the maximum observed in the Northern Hemisphere during the 1971 major warming). Zonal mean temperatures increased by about 10 K, with the maximum rise at 60° S, and were accompanied by simultaneous cooling between 20° S and 40° N with a maximum dip of 2.7 K in the tropics, indicating temporary changes of the global meridional circulation induced by the warming.

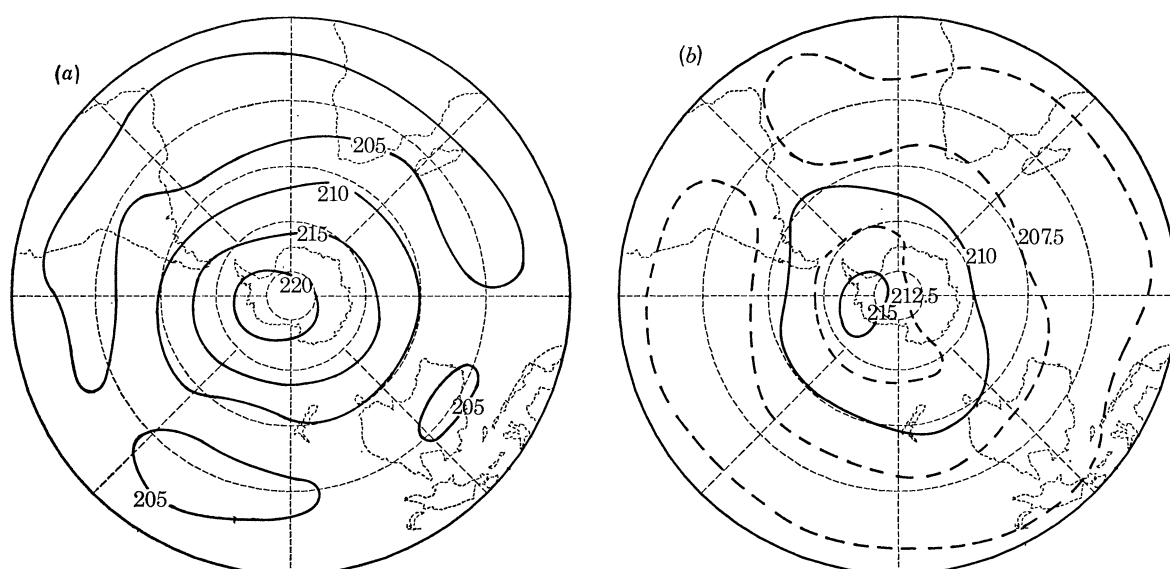


FIGURE 9. Change in temperature structure near 87 km using channel 3000 as in figure 8 from (a) July 1975 to (b) September 1975.

TABLE 1. LONGITUDES (°E) OF THE WAVENUMBER ONE RADIANCE MAXIMUM

	A2D		B4		B34		B12		2115 1975	2100 1975	3000 1975
	1973	1974	1973	1974	1973	1974	1973	1974			
May	160	220	110	140	50	110	340	40	†	†	†
June	170	+	110	+	40	+	0	+	†	†	†
July	190	180	90	80	60	30	20	10	80	270	270
Aug.	140	180	70	150	30	70	340	20	350	300	240
Sept.	100	160	70	80	40	40	290	30	20	330	250
Oct.	160	120	130	90	80	0	10	310	70	40	230
mean‡	154		95		44		354		40	325	248

+ Amplitude so small that phase not significant.

† Before launch.

‡ Excludes May and June.

2.4 *The mean eddy field*

Figure 8*a-c* shows the spatial structure of radiance measured by the p.m.r. during August 1976. There is a marked asymmetry about the pole at each level, and the wave is seen to tilt towards the west with increasing height. The pattern is almost completely wavenumber one with the greatest amplitude at the lowest level, near 43 km. Figure 9 shows that radiance fields at the top level were very similar in July, August and September, the warm centre being displaced towards 90° W in each case. Table 1 gives the longitudes of the temperature maxima at 60° S for all three channels and for s.c.r. observations in previous years. We are led to the conclusion that the mean wave occurs at approximately the same longitude each month and tilts westward with height from the tropopause to the mesopause with a 270° phase change, the slope being uniform over the whole range. An example of such a wave on a single day (24 August 1975) was given by Austen *et al.* (1976).

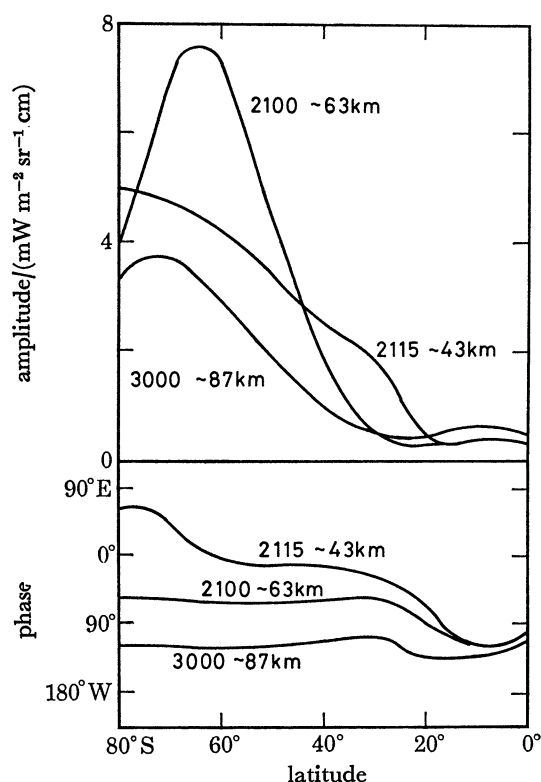


FIGURE 10. Structure of the offset vortex: amplitude and phase of the wavenumber one temperature wave averaged over August 1975. Phase is longitude eastward of the radiance maximum. One radiance unit of amplitude corresponds to ~ 0.87 K.

Although not obvious in figures 8 and 9 there are also definite phase changes with latitude, as shown in figure 10. S.c.r. data have shown that the wave axis is almost invariably tilted further west towards the equator in both hemispheres during winter (see Barnett 1975*a*) but figure 10 shows that such was not the case at higher levels in August 1976. July (not shown) was very similar with a marked tilt of similar magnitude near 43 km but no significant tilt near 85 km, but in September (not shown) both levels had a similar tilt of about 80° longitude between 80° S and 20° S.

CONCLUSION

A wide range of techniques are used to observe the atmosphere from spacecraft and have special value in remote parts of the globe where ground based measurements are sparse. However there are still major shortcomings: there are no measurements of atmospheric pressure, no routine observations of wind; temperature soundings have a vertical resolution which is substantially poorer than desirable in the troposphere, while soundings to the surface are impossible under continuous cloud cover. However many of the satellite data already obtained for the antarctic zone have not been studied and virtually no comparisons with surface-based observations have been made. The latter merits serious attention particularly where the method of satellite data reduction involves an atmospheric model which may need to be different in the Southern Hemisphere. A more comprehensive review of satellite observations of the atmosphere has been given by Houghton & Taylor (1973).

The s.c.r. and p.m.r. instruments have made temperature observations of the stratosphere for over 6 years and of the mesosphere for one year, and have clarified the behaviour of the atmosphere in the Southern Hemisphere. The standing planetary wave of wavenumber one (the offset vortex), previously observed in the stratosphere and generally supposed to be forced from the troposphere by the same variations that cause the cloud bands of figure 1, has been shown to propagate to the mesopause. Thus a means by which tropospheric and surface variations can affect ionospheric levels has been demonstrated. The behaviour of other wave modes awaits further investigation.

I wish to acknowledge the help of members of the Department of Atmospheric Physics and of the Nimbus project of N.A.S.A., and of Mr W. R. Piggott of the British Antarctic Survey for valuable comments on the manuscript. This research is supported by the Science Research Council and the Natural Environmental Research Council; N.A.S.A. has provided spacecraft and data handling facilities.

REFERENCES (Barnett)

- Adler, R. F. 1975 Mean meridional circulation in the Southern Hemisphere stratosphere based on satellite information. *Jl Atmos. Sci.* **32**, 893–898.
- Austen, M. D., Barnett, J. J., Curtis, P. D., Morgan, C. G., Houghton, J. T., Peskett, G. D., Rodgers, C. D. & Williamson, E. J. 1976 Satellite observations of planetary waves in the mesosphere. *Nature, Lond.* **260**, 594–596.
- Barnett, J. J. 1974 The mean meridional behaviour of the stratosphere from November 1970 to November 1971 derived from measurements by the selective chopper radiometer on Nimbus 4. *Q. Jl r. met. Soc.* **100**, 505–530.
- Barnett, J. J. 1975a Hemispheric coupling – evidence of a cross-equatorial planetary wave-guide in the stratosphere. *Q. Jl r. met. Soc.* **101**, 835–845.
- Barnett, J. J. 1975b Large sudden warming in the Southern Hemisphere. *Nature, Lond.* **255**, 387–389.
- Chapman, W. A., Cross, M. J., Flower, D. A., Peckham, G. E. & Smith, S. D. 1974 A spectral analysis of global atmospheric temperature fields observed by the selective chopper radiometer on the Nimbus 4 satellite during the year 1970–1. *Proc. R. Soc. Lond. A* **338**, 57–76.
- Curtis, P. D., Houghton, J. T., Peskett, G. D. & Rodgers, C. D. 1974 Remote sounding of atmospheric temperature from satellites. V. The pressure modulator radiometer for Nimbus F. *Proc. R. Soc. Lond. A* **337**, 135–150.
- Fletcher, J. O. 1975 The cryosphere. CIAP Monograph 4, pp. 4–39 to 4–50. U.S. Dept of Transport DOT-TST-75-54.
- Fritz, S. & Soules, S. D. 1972 Planetary variations of stratospheric temperatures. *Mon. Weath. Rev.* **100**, 582–589.
- Gloersen, P., Wilheit, T. T., Chang, T. C., Nordberg, W. & Campbell, W. J. 1974 Microwave maps of the polar ice of the Earth. *Bull. Am. Met. Soc.* **55**, 1442–1448.
- Harwood, R. S. 1975 The temperature structure of the Southern Hemisphere stratosphere August–October 1971. *Q. Jl r. met. Soc.* **101**, 75–91.

- Houghton, J. T. & Smith, S. D. 1970 Remote sounding of atmospheric temperature from satellites. I. Introduction. *Proc. R. Soc. Lond. A* **320**, 23–33.
- Houghton, J. T. & Taylor, F. W. 1973 Remote sounding from artificial satellites and space probes of the atmospheres of the Earth and the planets. *Rep. Prog. Phys.* **36**, 827–919.
- Krueger, A. J., Heath, D. F. & Mateer, C. L. 1973 Variations in the stratospheric ozone field inferred from Nimbus satellite observations. *Pure appl. Geophys.* **106–108**, 1254–1263.
- Labitzke, K. & Van Loon, H. 1972 The stratosphere in the Southern Hemisphere. Chapter 7 of *Meteorology of the Southern Hemisphere* (ed. C. W. Newton). Meteorological Monographs, vol. 13, no. 35. American Met. Soc.
- Morel, P. & Bandeen, W. 1973 The Eole experiment: early results and current objectives. *Bull. Am. Met. Soc.* **54**, 298–306.
- Krishna Rao, P. & McClain, E. P. 1974 Images from the NOAA-3 very high resolution radiometer over the North Sea and adjoining countries. *Weather* **29**, 436–442.
- Streten, N. A. 1973 Some characteristics of satellite-observed bands of persistent cloudiness over the Southern Hemisphere. *Mon. Weath. Rev.* **0101**, 486–495.
- Vonder Haar, T. H. & Suomi, V. E. 1971 Measurements of the Earth's radiation budget from satellites during a five-year period. Part 1: Extended time and space means. *J. atmos. Sci.* **28**, 305–314.